Hydrological Sciences Journal

ISSN: (Print) (Online) Journal homepage: https://www.tandfonline.com/loi/thsj20

Design flood hydrographs: a regional analysis based on flood reduction functions

Daniele Ganora, Giulia Evangelista, Silvia Cordero & Pierluigi Claps

To cite this article: Daniele Ganora, Giulia Evangelista, Silvia Cordero & Pierluigi Claps (2023) Design flood hydrographs: a regional analysis based on flood reduction functions, Hydrological Sciences Journal, 68:2, 325-340, DOI: 10.1080/02626667.2022.2153051

To link to this article: https://doi.org/10.1080/02626667.2022.2153051

HYDROLOGICAL SCIENCES JOURNAL
2023, VOL. 68, NO. 2, 325–340
https://doi.org/10.1080/02626667.2022.2153051

Design flood hydrographs: a regional analysis based on flood reduction functions

Daniele Ganora[a], Giulia Evangelista[a], Silvia Cordero[b] and Pierluigi Claps[a]

[a]Department of Environment, Land and Infrastructure Engineering, Politecnico di Torino, Torino, Italy; [b]Agenzia Interregionale Po, Ufficio periferico di Torino, Moncalieri, Italy

ABSTRACT

Modern flood hazard mapping techniques and water infrastructure design require the entire flood hydrograph. However, statistical methods for flood hydrograph estimation in ungauged basins have not received the same attention as the models used to predict the peak flow value. Here the design hydrograph of an ungauged basin is reconstructed in a parsimonious way through the estimation of a non-dimensional flood reduction function (FRF). Based on data from 87 basins (763 station-years of flood hydrographs), we show that a two-parameter FRF can be efficiently estimated by multiple linear regression from the longest drainage path length and slope of the basin, the average basin elevation, the width function kurtosis and the mean value of the scaling exponent of the intensity–duration–frequency curve. Reasonable similarities between the estimated flood hydrograph and the original ones make the method suitable for extension into other areas to estimate design hydrographs in ungauged basins.

ARTICLE HISTORY
Received 19 April 2022
Accepted 13 October 2022

EDITOR
A. Castellarin

ASSOCIATE EDITOR
K. Kochanek

KEYWORDS
volume of design hydrograph; flood reduction function; flood volume regionalization

1 Introduction

Modern hazard and flood risk analysis, used in the design of flood mitigation infrastructures, must be based on reliable information about hydrograph volume and shape, in addition to the peak flow value. However, while the estimation of design flood peaks has a long history (Gumbel 1945, Cunnane 1988, Castellarin *et al.* 2012) and many operational models are currently available, methods to estimate flood volume (and hydrograph shape) are still limited and not well consolidated (see e.g. Brunner *et al.* 2017, Tomirotti and Mignosa 2017), particularly in ungauged basins. In those cases, the lack of direct observations of historical flood volumes means that complex statistical estimation approaches are required. Basically, two main alternatives are found in the literature: on the one hand, it is possible to use indirect methods based on a rainfall input and a rainfall-runoff transformation to generate the hydrographs; on the other hand, regional statistical methods can be used to transfer information (e.g. the shape parameter of the hydrograph) from gauged to ungauged sites (see e.g. Blöschl *et al.* 2013). For this latter approach quite few examples are currently available, as most of the literature on the statistical analysis of peak and volume data refers to applications in gauged basins.

Several different implementations exist for the indirect methods, but they can be primarily classified into event-based or continuous simulation approaches (Ayalew *et al.* 2022). In the first case, a design hyetograph is preliminary defined and used as input in a rainfall-runoff model (e.g. Petroselli and Grimaldi 2018), while in the latter case one or more long-term rainfall records are used to generate a long record of synthetic hydrographs (e.g. Mediero *et al.* 2010, Grimaldi *et al.* 2022), and a subsequent statistical analysis of the synthetic hydrograph record allows the user to obtain the flood design parameters of interest (peak, volume, duration).

Indirect methods are often preferred over direct statistical estimation methods because rainfall records are generally quite long and have uniform geographical density while hydrometric records are shorter, non-uniform in space, and often include only annual maximum peak flows. Even if the hydrograph tracks are available, they are often recorded on paper (as is the case of Italy) and the required digitalization efforts make them difficult to obtain. With a very limited availability of flood volume data in many countries, it is no wonder that regional statistical characterizations of such complex curves are rare, resulting in a very fragmented literature on the subject with methods not easily applicable to other contexts. However, the direct statistical methods have the advantage of avoiding a rainfall-runoff transformation that introduces further uncertainties, and most of them take into account that flood peaks and flood volumes are positively correlated. This issue has been extensively investigated: Yue *et al.* (1999), for instance, suggested jointly modelling the peak and volume with a multivariate distribution. In the same vein we find the copula-based bivariate modelling of peak and volume developed by Zhang and Singh (2006), Salvadori and De Michele (2007), Bacova Mitková and Halmová (2014), or Requena *et al.* (2016), among others. Most of these approaches, when directed to the estimation of the design hydrograph, leave the definition of the hydrograph shape to a subjective choice (e.g. triangular, rectangular, etc.) while focusing on a limited number of hydrograph

CONTACT Giulia Evangelista giulia.evangelista@polito.it Department of Environment, Land and Infrastructure Engineering, Politecnico di Torino, Corso Duca degli Abruzzi 24, Torino 10129, Italy

characteristics. An exception is the procedure developed by Yue *et al.* (2002), which reproduces the hydrograph shape in a statistical way provided that design values of peak flow, volume and duration are available. In principle, this approach could be combined with the previously cited ones to include the shape among the design flood features. Another approach considering the hydrograph shape is that of Brunner *et al.* (2017), who use a dimensionless lognormal probability distribution, scaled according to flood peak and volume values, modelled through a bivariate copula.

A different and less common approach to characterize the flood volumes in a design hydrograph procedure relies on the use of the flood reduction function (FRF; e.g. Bacchi *et al.* 1992). The idea is to use a parsimonious function to represent how the flood volume is distributed for a given duration, where a duration of zero corresponds to the peak value. The FRF curve is conceptually similar to the average intensity–duration–frequency (IDF) function used to represent rainfall depths for a given duration (Grimaldi *et al.* 2011). Strictly speaking, the method does not account for the shape of the hydrograph, but provides a duration–volume constraint that allows the users to reconstruct a meaningful synthetic hydrograph using only a few parameters and simple hypotheses about the shape.

As our investigation is directed towards developing a regional statistical method for the estimation of the design hydrograph in ungauged basins, we have considered that the FRF paradigm has the right characteristics of simplicity and parsimony to be applied in contexts of limited availability of data. In this paper we consider the FRF paradigm using a parametrization with a simple two-parameter function, known as the Natural Environment Research Council (NERC) equation, that can be estimated also in ungauged basins through regional analysis. The proposed methodology is built using a dataset of flood volumes of 87 basins in the upper Po River basin, northwest Italy, which is a much larger dataset than those used in previous applications (see e.g. the regionalization experiment, also based on the FRF, by Maione *et al.* 2003).

The proposed methodology is conceived to be tightly connected to available regional models for the estimation of the flood peaks, and to be easily adapted to other geographical contexts.

2 Methodology

2.1 Flood reduction function

FRF is a curve representing, for a given duration D, the maximum value of the average discharge Q_D computed for all the possible time windows of duration D over a period of interest. The curve is usually normalized by the instantaneous maximum discharge, Q_{PEAK} (i.e. considering D = 0), of the same period as:

$$\varepsilon_D = \frac{Q_D}{Q_{PEAK}} = \frac{1}{Q_{PEAK}} \max\left(\frac{1}{D}\int_t^{t+D} Q(\tau)d\tau\right) \quad (1)$$

In practical applications the period of interest for the selection of maxima is usually the year and the observations of Q are recorded at discrete time steps (e.g. 10 minutes). For a specified value of D, ε_D is also referred to as the "flood reduction ratio." Following the classical approach used for flow duration curves and IDF curves (Chow 1951), the empirical FRF is computed for all the available years, normalized by the corresponding annual maximum. Subsequently, the values are averaged over the years, to obtain a basin representative $\overline{\varepsilon_D}$ curve (see Fig. 1(b)) to be used in practical applications.

Over the years, for each duration D, one computes a sample of $\overline{\varepsilon_{Dj}}$ values (j = 1 ... N) so that a statistical treatment would enable to estimate a quantile $\varepsilon_{D,T}$. This can be done for each duration and, in principle, the probability distribution may vary among durations. However, it has been shown (Franchini and Galeati 2000) that it is generally acceptable to use a unique probability distribution for all durations D. This enables us to use a simple expression for the estimation of the quantile of the flood volume for design purposes, as follows:

$$W_{D,T} = \bar{\varepsilon}_D Q_T D \quad (2)$$

In Equation (2) Q_T is the quantile of the flood peak for a given return period, that can be represented as $Q_T = \bar{Q} \cdot K_T$ according to the index method (Dalrymple 1960). This entails that the non-dimensional probability distribution of flood peaks, K_T, is adopted as the non-dimensional distribution of the flood volumes, regardless of the duration D of interest.

Equation (2) can be used to build synthetic design hydrographs by derivation of the volume function:

$$\hat{Q}(t) = \frac{dW}{dt} = Q_T \cdot \overline{\varepsilon_D} + t \cdot Q_T \cdot \overline{\varepsilon_D}' \quad (3)$$

where $\hat{Q}(t)$ is the synthetic hydrograph and $\overline{\varepsilon_D}'$ indicates the first derivative of ε with respect to the duration *D*. It is important to stress the conceptual difference between the chronological time *t* and the duration *D*, the latter being essentially a moving time window.

According to the UK National Environmental Research Council (Natural Environment Research Council 1975), the average FRF can be represented by a two-parameter curve:

$$\varepsilon_D = \frac{Q_{D,T}}{Q_T} = (1 + b \cdot D)^{-c} \quad (4)$$

where *b* and *c* are parameters to be determined. The dependence on the return period is, again, only concentrated in the peak flow Q_T, so that the form of the curve (Equation 4) is independent of the return period.

In the scientific literature, other analytical forms of the FRF have been proposed: Franchini and Galeati (2000) compared different analytical models (the NERC, the geomorphoclimatic model by Fiorentino *et al.* 1987, the stochastic model by Bacchi *et al.* 1992) against the empirical FRFs of 12 basins in central Italy. All the models showed a reliable fitting to the observed FRF, although the geomorphoclimatic model was more complex to apply. As the NERC function allows double curvature and it is compatible with a conceptual framework (see Section 2.2), we consider the NERC to be the best choice for an analytical FRF to

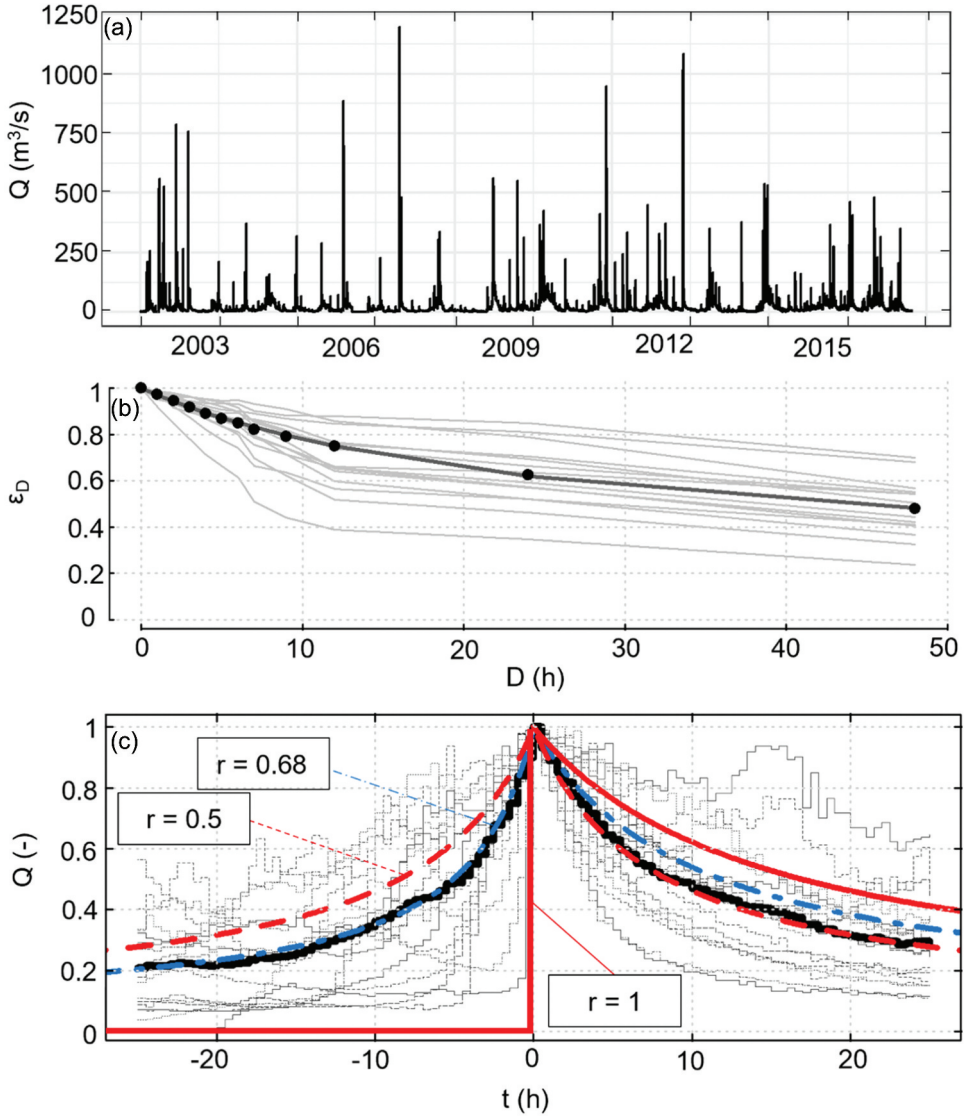

Figure 1. Example of flood reduction function hydrograph analysis for the Stura di Lanzo at Torino basin. (a) Time series of discharge values recorded at 30min resolution. (b) Empirical annual flood reduction functions (thin lines), empirical average flood reduction function (dots) and Natural Environment Research Council analytical flood reduction function (b = 0.05627, c = 0.55830). (c) Natural Environment Research Council hydrograph obtained from flood reduction function of panel (b) with r = 0.68 (dot-dashed line) compared to the reference hydrograph (bold solid line) and the single event observed hydrographs (thin lines). Dashed and solid thin curves show the symmetrical Natural Environment Research Council hydrograph (r = 0.5) and Natural Environment Research Council hydrograph with instantaneous initial peak (r = 1), respectively.

be regionalized, although the results obtained in this work can be easily generalized to other kind of functions.

Summarizing, one can use the empirical FRF at a gauged location and Equation (3) to obtain a single representative form as a design hydrograph. The procedure can be summarized with a few steps (sketched in Fig. 1):

(1) starting from a discharge time series (Fig. 1(a)) for each year, the empirical FRF of Equation (1) can be computed by considering different time windows (Fig. 1(b), thin lines);
(2) the average empirical FRF is then obtained by averaging the individual values for each duration (Fig. 1(b), dots);
(3) the analytical NERC model (Equation 4) is fitted to the average FRF, providing an analytical representation of the FRF (Fig. 1(b), solid line);
(4) a synthetic hydrograph consistent with Equation (4) can be built from the fitted FRF.

To apply step 4, it is first necessary to define the peak position as, with respect to the duration D, if the peak is at t = 0, the hydrograph shape is that represented as a solid thin line in Fig. 1(c). To derive the hydrograph with peak at t=0, combining Equations (3) and (4), we obtain:

$$\hat{Q}(t) = Q_T \cdot \left[(1+bt)^{-c} - cbt(1+bt)^{-c-1}\right] \tag{5}$$

Considering two asymmetrical limbs, a more general analytical form of the hydrograph shape can be written as:

$$\hat{Q}(t)\begin{cases} \left(1+\frac{b}{1-r}|t|\right)^{-c} - \frac{b\cdot c}{1-r}|t|\left(1+\frac{b}{1-r}|t|\right)^{-c-1} t<0 \\ \left(1+\frac{b}{r}t\right)^{-c} - \frac{b\cdot c}{r}t\left(1+\frac{b}{r}t\right)^{-c-1} t\geq 0 \end{cases} \tag{6}$$

where the shape depends on the "skew" parameter r ($0 \leq r \leq 1$). The symmetrical hydrograph (with central peak) is generated from Equation (6) with r = 0.5. The "initial peak" hydrograph is obtained with with r = 1. An example of asymmetrical shape is the dot-dashed curve shown in Fig. 1(c), obtained with r = 0.68. Of course, both the hydrograph forms are consistent with the same FRF (i.e. Equations (5) and (6) lead to the same εD values) when recomputing the volumes over moving time windows.

Some authors (Tomirotti and Mignosa 2017) let the *r* parameter vary with the hydrograph duration, after considering various real hydrographs on large rivers. In this study, the parameter *r* is considered constant for each basin, i.e. it is independent of *D*. The reasons of this choice are discussed later. It should also be clarified that here, unlike in the work by Tomirotti and Mignosa (2017), the skew parameter r represents the ratio between the time after the peak and the duration D.

A specific analysis of the hydrograph shape is offered in Section 5.1, as an additional validation to the proposed method.

Basically, the regionalized methods presented in this paper address step 3 of the above procedure in ungauged basins. The following section provides the theory, and in Section 3 the application in northwest Italy demonstrates the feasibility.

2.2 Estimation of the FRF in ungauged basins

As mentioned in the Introduction, while regionalization of peak flow values is a consolidated practice, with many procedures available, much less can be found in the literature as regards the regionalization of other hydrograph-related characteristics. Something different from the regionalization of peaks can be found in NERC (1975), where the non-dimensional (with respect to the mean annual daily flood) FRF values at three and 10 days (AR3 and AR10, respectively) were related to catchment characteristics through linear regressions. The analysis was based on a sample of 64 stations and an initial set of four catchment descriptors; the final regional models to estimate AR3 and AR10 both proved to be a function of the stream slope. Much later, another approach was proposed by Maione *et al.* (2003), and later followed by Tomirotti and Mignosa (2017), for the regional estimation of the FRF (which stood for flood duration frequency in the original paper). Maione *et al.* (2003) used a single-parameter FRF (Bacchi *et al.* 1992) to correlate this parameter to the watershed area using a linear regression fitted on eight gauged basins in the Po basin (Italy) with 46 years of average record length. More recently, Brunner *et al.* (2018) tested different approaches for regionalization of a synthetic normalized hydrograph shape. A total of 24 approaches were tested to estimate the 10 parameters of a synthetic design hydrograph form proposed in the paper. They were linear regression techniques; non-linear regression models, i.e. random forest, bagging and boosting; spatial proximity approaches; and methods based on homogeneous regions. Strictly speaking, the FRF concept was not used.

The foundations of the procedures proposed here lie in a conceptual interpretation of the NERC FRF proposed by Silvagni (1984) who connected parameters *b* and *c* of the NERC curve to the parameters of the rational formula (Mulvaney 1851). In practice, assuming that the peak Q_T can be estimated considering a rectangular design rainfall over the basin, with duration equal to the time of concentration t_c, Silvagni (1984) suggested that $Q_{D,T}$ could also be estimated through the rational formula but using a rainfall event having duration t_c+*D*. Assuming that the design rainfall intensity $i_T(d)$ for a given duration d and return period T can be expressed using a two-parameter IDF curve $i_T(d) = a_T d^{n-1}$ (e.g. Koutsoyiannis *et al.* 1998), the author obtained a "rational" FRF expression as:

$$\varepsilon_D = \frac{Q_{D,T}}{Q_T} = \frac{i_T(t_c + D)\,A\varphi}{3.6}\left(\frac{i_T(t_c)A\varphi}{3.6}\right)^{-1} = \frac{a_t.(t_c + D)^{n-1}}{a_t.{t_c}^{n-1}} = \left(1 + \frac{D}{t_c}\right)^{n-1}, \tag{7}$$

where A is the basin area and φ is the runoff coefficient. Comparing Equation (7) with Equation (4), one can recognize that the parameters of the NERC FRF can assume the meaning of:

$$b = \frac{1}{t_c}\, e\, c = 1 - n. \tag{8}$$

Equations (4) and (8) can be used, in principle, to estimate *b* and *c* from only the IDF parameter *n* and the time of concentration t_c. By inverting the procedure, Franchini and Galeati (2000, 170) observed that when using several empirical FRFs to estimate t_c, with the conceptual analogy of Silvagni (1984), the results were significantly different from those obtained by estimating t_c with the most common equations in the literature. They suggested that the parameter *b* of the NERC equation cannot be directly linked to the usual basin time of concentration. Rather, 1/*b* should be interpreted "as a more general 'reference time,' characteristic of the response of the basin" in the FRF framework. In the following, we will thus refer to the parameter 1/*b*, whose values can be referred to an intuitive meaning of "t_c."

The method of regional analysis proposed here is essentially built through the institution of relations between the two parameters of the NERC FRF and several basin characteristics. Three regional statistical approaches are applied to an extensive dataset of hydrographs and flood reduction curves, to allow the estimation of the FRF parameters in ungauged basins. The methods considered are: multiple linear regression (LR; e.g. Montgomery *et al.* 2001), canonical correlation analysis (CCA; e.g. Ouarda *et al.* 2000) and the alternating conditional expectation algorithm (ACE; e.g. Breiman and Friedman 1985a and 1985b). In all the techniques the basin characteristics, referred to as descriptors, include geographical, morphological and climatic basin attributes. These are related to the basins upstream of the available gauging stations and can be easily computed in any ungauged basin by means of Geographic Information System (GIS) procedures.

For each regionalization approach tested, several alternative models, based on different subsets of descriptors, have been implemented, and subsequently ranked, according to their prediction performances, e.g. by the adjusted coefficient of determination (R^2_{adj}). The most significant models are further

validated with a visual checking of the results, and with a leave-one-out cross-validation procedure (see Hastie *et al.* 2009). In the following, the details of the applications are presented, and a final assessment of the most convenient method is discussed.

2.2.1 Multiple linear regression

Multiple linear regressions have been widely used to regionalize hydrological variables. An example of a prediction equation is:

$$\hat{y} = \beta_0 + \beta_1 \chi_1 + \cdots + \beta_p \chi_p \tag{9}$$

where $\hat{y}$ is the (FRF) parameter to regionalize, x is a basin descriptor and β is its corresponding regression coefficient. In this work, the ordinary least squares method (e.g. Montgomery *et al.* 2001) is used and the model considers both the NERC parameters b and c as the regionalized variable $\hat{y}$. Different possible transformations (log, Box-Cox; Box and Cox 1964) have been considered for both the variable sets x and y, e.g. considering $y = c$ and $y = b$ or $y = ln(b)$ or $y = 1/b$ or $y = ln(1/b)$. Only the most significant results are reported here, and, for instance, no transformation of c has provided satisfactory results.

Regarding the covariates x, a preliminary analysis of their frequency distribution showed that some of them are markedly skewed, and that the logarithmic and Box-Cox transformation can be effective to correct the skewness. For each set of transformations (on y and x), all the possible combinations of two and three descriptors have been computed, producing about 6000 combinations. Using the obtained results, the regression models are tested for significance (Student's t-test at 5%), multicollinearity (Variance inflation factor (VIF) test; see Montgomery *et al.* 2001) and residual analysis (normal probability plot and homoscedasticity). The subset of results passing all the tests are then ranked according to the R^2_{adj} computed on the variables back-transformed to their original units. Section 3.2 of this paper thoroughly describes the results of applying this procedure.

2.2.2 Canonical correlation analysis

CCA is a method used to explore relationships between two multivariate sets of variables, that are here represented by FRF parameters (b^{-1} and c) and by the basin descriptors. The CCA allows one to determine which is the linear combination of the variables of the latter group most correlated to a linear combination of the variables of the former group. CCA is widely used in statistics: e.g. multivariate regression and factorial discriminant analysis are special cases of the CCA method (Ouarda *et al.* 2001). Approaches belonging to this family have been commonly applied in hydrology since the works of Snyder (1962) and Wong (1963). More recently, Ouarda *et al.* (2000) developed a CCA-based procedure to assess the joint regional estimation of spring flood peaks and volume for Northern Canadian basins.

To resume the functioning of the CCA, let $\mathbf{X}$ be the $n \times p$ matrix of basins descriptors, where n is the number of basins in the dataset and p is the number of the considered descriptors, and let $\mathbf{Y}$ be the $n \times 2$ matrix of the FRF parameters. The predicted parameters $\hat{y} = \left[\hat{\frac{1}{b}}\ \hat{c}\right]$ can be computed as

$$\widehat{\mathbf{Y}} = \varrho \cdot [\boldsymbol{x} - \overline{\boldsymbol{x}}]\mathbf{A} \cdot \mathbf{B}^{-1} + \overline{\mathbf{Y}} \tag{10}$$

where the descriptors of the ungauged basin are included in vector $\mathbf{x}$ while each column of $\overline{\boldsymbol{x}}$ is the mean value of the corresponding descriptors in $\mathbf{X}$, computed from the n gauged basins of the calibration dataset. Similarly, $\overline{\mathbf{Y}}$ is the vector of mean values of the FRF parameters computed from the n gauged basins of the dataset. Two matrices of canonical variables are defined: $\mathbf{U} = [\boldsymbol{x} - \overline{\boldsymbol{x}}]\boldsymbol{A}$ and $\mathbf{V} = [\boldsymbol{Y} - \overline{\boldsymbol{Y}}]\mathbf{B}$. The canonical correlation between the j^{th} pair of canonical variables is then:

$$\varrho = \frac{cov(u_j, v_j)}{\sqrt{var(u_j)\, var(v_j)}} \tag{11}$$

Matrices A and B contain the canonical coefficients a_j and b_j, scaled to make the covariance matrices of the canonical variables the identity matrix, and ϱ is the square root of the corresponding eigenvalue (Ouarda *et al.* 2001).

The aim of the CCA is thus to find the coefficients a and b that maximize ϱ. The results of the CCA application are reported later, in Section 3.3.

2.2.3 Alternating conditional expectation algorithm

The ACE algorithm was proposed by Breiman and Friedman (1985a, 1985b) as a non-parametric model to find those transformations that produce the best-fitting additive model. Considering y and $x_1, \ldots, x_p$ as the response and the predictor random variables, respectively, the ACE algorithm provides a mapping function t for each variable, which defines a set of non-parametric transformations. The prediction variable is then obtained as

$$\hat{y} = t_y^{-1}\left[t_{x_1}(x_1) + t_{x_2}(x_2) + \ldots + t_{x_p}(x_p)\right] \tag{12}$$

where t_y^{-1} is the inverse of the mapping function of the variable y, and t_{xi} is the mapping function of the i^{th} descriptor. The optimal transformations are achieved through an iterative series of optimizations. While the reader can refer to Breiman and Friedman (1985a and 1985b) for the algorithm details, it is worth recalling the practical procedure through a graphical example presented in Fig. 2: after the mapping functions have been computed, the two descriptors x_1 and x_2 of the ungauged basin are entered in the respective mapping functions to obtain their transformed values; their sum is then back-transformed with the t_y mapping function to obtain the final estimate.

With respect to the linear regression, the ACE approach can automatically detect possible efficient non-linear transformation of the variables (both x and y), so that no preliminary transformations are applied. The mapping function t_y is here forced to be linear, to ensure a more robust inversion of t_y; no constraints are applied to the descriptors instead. All the numerical analyses have been performed with the R package "acepack" (Spector *et al.* 2016). The results of the ACE application are reported in Section 3.4.

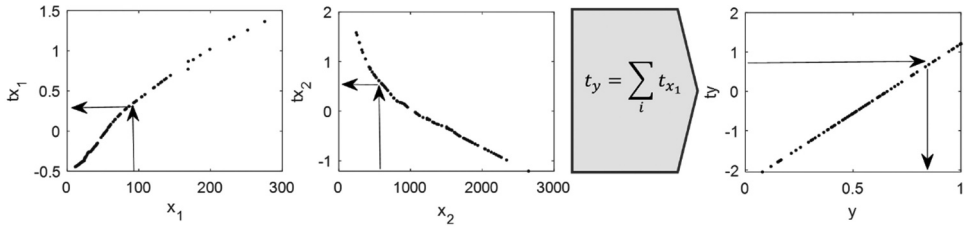

Figure 2. Example of Alternating Conditional Expectation algorithm application: x_1 and x_2 are two independent variables and tx_1 and tx_2 are their non-parametric transformations; y is the dependent variable obtained as the back-transformation of t_y. The mapping functions are represented by black dots as they are computed for each sample value.

3 Case study and regional model building

3.1 Case study and data preparation

The methodologies presented in the previous section were used to build regional models of the FRF curves in an area of about 25 000 km^2 in the northwest of Italy. The case study was organized by assembling a new dataset of flood hydrographs, extracting flood waves from the continuous discharge time series originally recorded in 87 gauging stations of the Regional Agency for Environmental Protection (ARPA Piemonte). The dataset was initially compiled using information available from previous, partially unpublished, studies that reported data manually collected by the former Italian Hydrographic Service. In particular, they consist in:

- 26 time series of hydrometric levels obtained from digitalization (at 15min) of data recorded by analogic gauges during the period 1928–1994. These water levels have been transformed into discharge values using previously obtained rating curves for these stations (Claps *et al.* 2010);
- FRFs obtained based on the three major events records in a single year (data digitalized from analogic recordings) for 18 gauges between 1928 and 1994.
- New data, from 2000 to 2015, available in digital format with a time resolution of 10min to 30min.

In all cases, annual records with more than 30% missing values in a single year were discarded. However, incomplete years (with less than 30% missing values) were further investigated: if no significant precipitation was found during or before the gap periods, the river was considered in low-flow conditions during these gaps and the record was considered reliable for flood hydrograph extraction.

Altogether, the dataset reaches a total of 87 gauging stations with at least six years of record each over the period 1928–2015, resulting in a total of 763 station-year records, with an average length of 15 years and a maximum length of 64 years. The spatial distribution of the gauges is shown in Fig. 3(a), while data availability over time is summarized in Fig. 3(b). All the data used in terms of annual FRFs, as well as the main characteristics of the 87 basins, are available in a web GIS (www.resba.it).

As a preparatory step for the regional statistical analyses, we computed the empirical mean annual FRFs in all of the 87 stations and then we fitted the empirical curves with the NERC model of Equation (4). The best-fitting curve was obtained by numerical least squares minimization, using the MATLAB® function "fit" (with the default "trust-region" algorithm; Moré and Sorensen 1983). Parameters b and c are then jointly estimated and constrained to be non-negative. The final fitting of the NERC curve to the empirical average FRF proved to be adequate for all the basins, with a mean coefficient of determination (R^2_{adj}) of 0.995.

For all 87 watersheds, almost 100 basin attributes were available, as already published by Gallo *et al.* (2013). The set of geomorphological descriptors was obtained by processing the National Aeronautics and Space Administration (NASA) SRTM (Shuttle Radar Topography Mission) Digital Elevation Model (Farr *et al.* 2007), sampled at a 100 m spatial resolution. A subset of descriptors to be used in the regional analyses was selected, as described in Appendix Table A1. The procedure for selecting subsets of descriptors is detailed in Cordero (2019).

3.2 Regional model calibration 1: multiple linear regression

In pursuing the goal to reconstruct the NERC parameters $1/b$ and c for ungauged basins, both were considered as prediction variables in multiple linear regressions. Observations of b and c were the values fitted to the average FRF curve for each station in the data preparation step discussed above.

All the possible combinations of two and three basin attributes (Appendix Table A1) were used as set of covariates in the multiple regressions, including some variants where $1/b$, c and the covariates were transformed. The best-performing models obtained are reported in Table 1, together with some goodness-of-fit indicators, i.e. the adjusted R-squared, R^2_{adj}, and the relative root mean squared error, $RRMSE = \frac{\sqrt{\sum \left(\hat{y}_i - y_i\right)^2 n^{-1}}}{\bar{y}}$. For operational purposes, when different models reached similar performances the preferred one has been that based on "simpler" descriptors (i.e. easier to compute). This is the case for models 1 and 2 in Table 1. Despite the high performance of the models subjected to Box-Cox transformation in limiting the skewness of residuals (see Cordero 2019), considering the overall performances, we suggest concluding with the choice of the models ID 1 and ID 5 of Table 1, where the log-transformation of the x variable is applied.

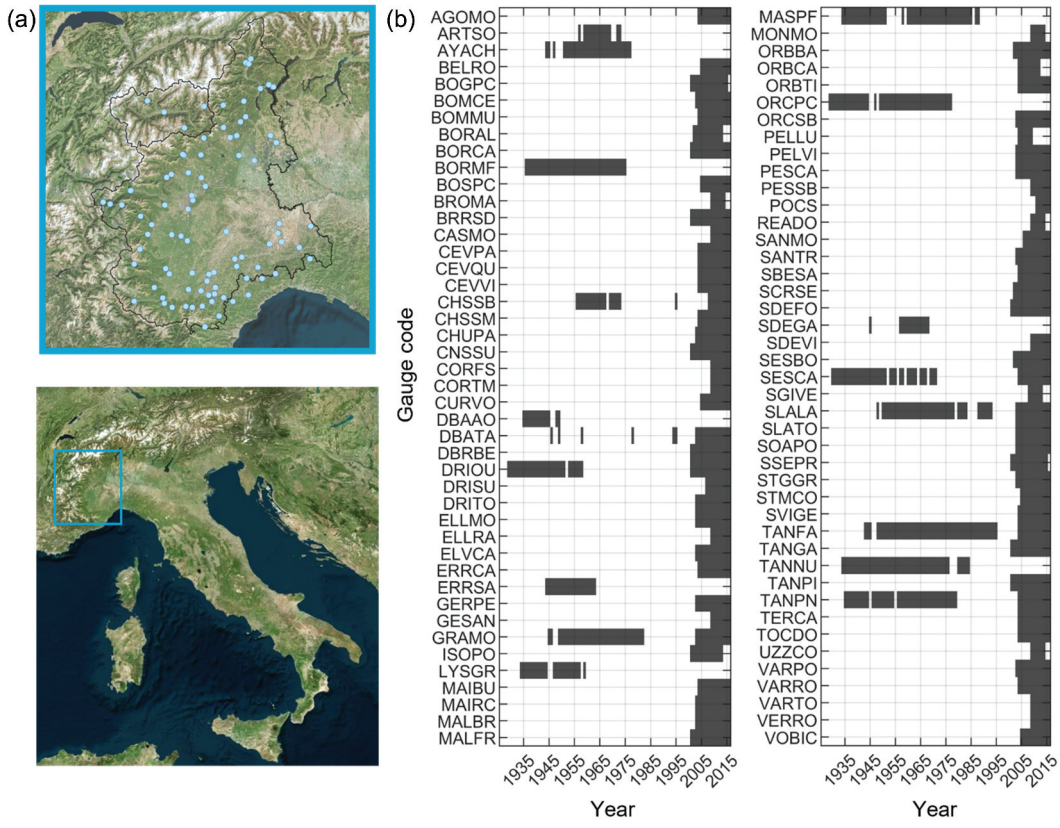

Figure 3. (a) Geographical location of the 87 gauging stations in the database. (b) Years with available data (after quality checks) for each gauge. Gauge codes allow us to access the watershed descriptors in Gallo *et al.* (2013) and in the web GIS mentioned in the main text.

Table 1. Best regionalization linear models for 1/b and c. From left to right: model identification, transformation applied to independent variables, number of independent variables, dependent variables (y), independent variables (x), coefficients (β), R^2_{adj} and RRMSE. The last two models refer to 1/b estimated directly from c. For the meaning of the symbols, see the Appendix.

ID	Transformation	No. descriptors	y	x	β	R^2_{adj}	RRMSE
1	Natural logarithm	3	c	ln (H_{avg}) ln (LDP) ln (IDFn)	4.8403 −0.58869 0.13813 0.80202	0.5879	0.40
2	Box-Cox	3	$c^{0.1635}$	$H_{avg}^{0.6938}$ $LDP^{-0.2929}$ $IDFn^{1.9984}$	1.1436 −0.0019 −0.3648 0.6423	0.5487	0.41
3	Natural logarithm	2	c	ln (H_{avg}) ln (LDP)	2.9990 −0.4190 0.1421	0.5626	0.42
4	Box-Cox	2	$c^{0.1635}$	$H_{avg}^{0.6938}$ $LDP^{-0.2929}$	1.1943 −0.0013 −0.3609	0.5417	0.41
5	Natural logarithm	3	ln(1/b)	ln (ku_{fa}) ln (LDP) ln (LDPs)	3.7285 −2.0775 0.5006 −0.7715	0.4287	0.74
6	Box-Cox	3	$(1/b)^{0.0851}$	$H_{avg}^{0.6938}$ $ku_{fa}^{0.5423}$ $LDP^{-0.2929}$	1.9611 −0.0008 −0.2048 −0.8146	0.3797	0.76
7	Natural logarithm	2	ln(1/b)	ln (H_{avg}) ln (LDP)	4.7943 −0.6859 0.6986	0.3491	0.79
8	Box-Cox	2	$(1/b)^{0.0851}$	$H_{avg}^{0.6938}$ $LDP^{-0.2929}$	1.6236 −0.0008 −0.7506	0.3311	0.80
9	b estimated from observed c		ln(1/b)	ln (c)	3.4589 1.2908	0.6190	0.61
10	b estimated from c estimated by model 1		ln(1/b)	ln ($\hat{c}$)	3.4589 1.2908	0.2856	0.84

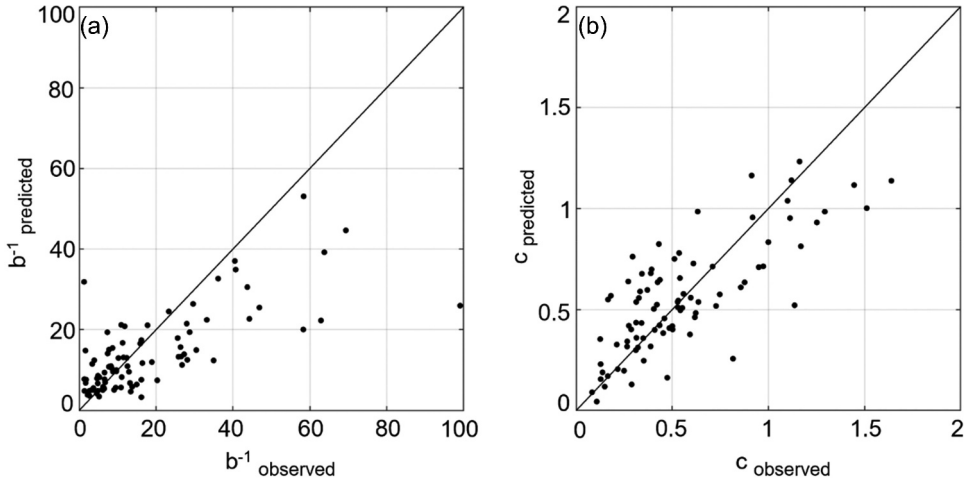

Figure 4. Estimated versus empirical values of parameters (a) 1/b and (b) c based on the linear regionalization model of Equations (13) and (14).

For both c and $1/b$, the descriptors emerging in the best regressions are substantially the same. It is also clear that, despite the high correlation between b^{-1} and c (see ID = 9 in Table 1), the most robust way to estimate b is not as a function of c, as shown in the results of ID = 10.

The best models found (ID = 1 for c and ID = 5 for b^{-1}) have the following expressions:

$$ln\left(\frac{1}{b}\right) = 3.7285 - 2.0775 \cdot ln\left(ku_{fa}\right) + 0.5006 \cdot ln(LDP) - 0.7715 \cdot ln(LDP_s) \quad (13)$$

$$c = 4.8403 - 0.58869 \cdot ln\left(H_{avg}\right) + 0.13813 \cdot ln(LDP) + 0.80202 \cdot ln(IDFn) \quad (14)$$

Again, the definitions of the descriptors are reported in Appendix Table A1. A graphical representation of the performances of Equations (13) and (14) is shown in Fig. 4, which reports a comparison between the observed and predicted FRF parameters.

3.3 Regional model calibration 2: CCA

The CCA method is applied considering again all the possible combinations of two and three descriptors. This time they have been reduced to a benchmark set that includes the 10 most robust and easy to compute descriptors selected by an iterative pruning procedure. This procedure deletes, at each iteration, the descriptors most correlated to each other. The set of 10 descriptors selected is reported in Table 2.

Figure 5 shows, for both parameters b^{-1} and c, the values obtained from the local estimates versus those obtained from the regional CCA estimate built using a 10-descriptor model. All the model coefficients (a_j, b_j and the mean values $\bar{x}_j$ and $\bar{y}_j$) are reported in Table 2. The fitting performances are R^2_{adj} = 0.4432 and RRMSE = 0.7314 for b^{-1}, and R^2_{adj} = 0.58 and RRMSE = 0.3993 for c.

Among the top 10 combinations that use only two or three descriptors (see Table 3), similarly to the number of independent variables used in the previous method, the most significant model from a hydrological and practical point of view is ranked eighth, based on the canonical correlation ϱ. For this model, the coefficients a_j and b_j, the mean values $\bar{x}_j$ and $\bar{y}_j$, and the canonical correlation ϱ are summarized in Table 4. However, R^2_{adj} and RRMSE are respectively −0.1 and 1.03 for b^{-1} and 0.39 and 0.48 for c, and the model is therefore not explanatory. Figure 6 shows the fitting performances of model 8 in Table 3.

3.4 Regional model calibration 3: ACE

For the ACE algorithm application, as in the case of multiple regressions, all the possible combinations of two and three

Table 2. Coefficients of the best CCA model based on 10 descriptors. The meaning of the descriptors is reported in the Appendix.

Descriptors	$\bar{x}_j$	a_1	a_2
A	430.68	$-5.1894 \cdot 10^{-4}$	$-5.8926 \cdot 10^{-5}$
H_{avg}	1290.50	$-1.4485 \cdot 10^{-3}$	$2.3539 \cdot 10^{-4}$
X_b	403 985.71	$6.2250 \cdot 10^{-6}$	$2.9468 \cdot 10^{-6}$
Y_b	4 976 076.19	$3.4813 \cdot 10^{-6}$	$1.7074 \cdot 10^{-6}$
D_d	0.64	1.3540	2.9862
LDP	44.04	$8.0066 \cdot 10^{-3}$	$2.2960 \cdot 10^{-2}$
MAP	1239.83	$-2.7431 \cdot 10^{-3}$	$-5.9138 \cdot 10^{-4}$
IDFa	24.03	0.1003	$-4.2900 \cdot 10^{-3}$
IDFn	0.46	11.9365	0.4314
c_f	0.44	−0.7036	−3.4828
	$\bar{y}_j$	$\mathbf{b_1}$	$\mathbf{b_2}$
1/b	18.5718	−0.0264	0.0865
c	0.5628	3.8355	−2.7990
ϱ		0.7781	

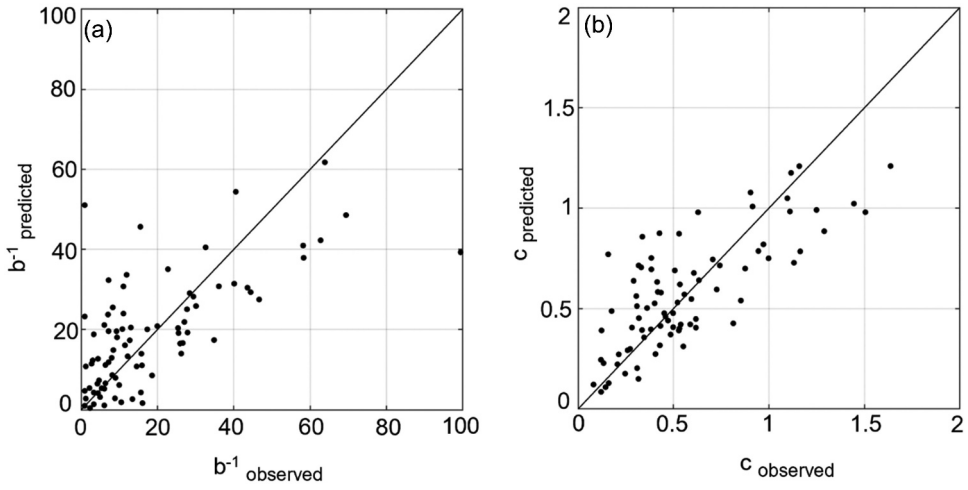

Figure 5. Values obtained from local estimates of (a) 1/b and (b) c versus those obtained from the Canonical Correlation Analysis regional model based on 10 descriptors (see Table 2).

Table 3. Top 10 combinations (ranked by the canonical correlation values) that use only two or three descriptors. The most significant model from a hydrological and practical point of view is highlighted.

Ranking	Descriptors	$\bar{y}_j$
1	H_{avg}, ku_{fa}, $Fourier_{B2}$	0.74699
2	H_{avg}, Lca_{12h}, cv[rr]	0.74650
3	H_{avg}, ku_{fa}, cv[MAP]	0.74586
4	H_{avg}, Lca_{3h}, cv[rr]	0.74253
5	H_{avg}, ku_{fa}, cv[rr]	0.74153
6	H_{avg}, ku_{fa}, IDFn	0.74109
7	H_{avg}, R_s, cv[rr]	0.74026
8	***H_{avg},R_s, IDFn***	***0.73923***
9	H_{avg}, ku_{fa}, Lca_{12h}	0.73903
10	H_{avg}, ku_{fa}, Lca_{3h}	0.73852

Table 4. Coefficients of the best Canonical Correlation Analysis model based on three descriptors. The meaning of the descriptors is reported in Appendix.

Descriptors	$\bar{x}_j$	a_1	a_2
H_{avg}	1290.50	−0.0023	0.0018
R_s	2.1834	−0.3847	−0.2578
IDFn	0.46	7.5196	−26.0262
	$\bar{y}_j$	$\mathbf{b_1}$	$\mathbf{b_2}$
1/b	18.5718	−0.0379	0.0821
c	0.5628	4.1778	−2.2565
ϱ		0.7392	

descriptors have been considered. Preliminary data transformations are not applied in this case, since the ACE algorithm already searches for an optimal transformation. The best models found for c and b^{-1}, ranked by R^2_{adj}, are listed in Table 5. The mapping functions of the highest performing models are shown in Fig. 7. Estimated values of b^{-1} and c are finally compared to the observed ones in Fig. 8. The results are quite interesting and are fully explored in the Discussion section.

4 Discussion

Before undertaking comparative analyses among the results obtained with the three methods applied, we point out that for all models the leave-one-out cross-validation procedure has been applied. The main goal is to check the correct reproduction of the observed mean FRFs, but some considerations are also applied to the form of the hydrographs.

First of all, the cross-validation has been applied to check the model performances in the reproduction of the FRF parameters, i.e. *1/b* and *c*. Considering the multiple LR models of Equations (13) and (14) and applying the leave-one-out cross-validation procedure, prediction performances worsen, as expected. For the parameter *1/b*, R^2_{adj} drops from 0.4287 to 0.3669 and the RRMSE rises from 0.74 to 0.78; for the parameter *c*, the R^2_{adj} changes from 0.5879 to 0.5374 and the RRMSE increases from 0.40 to 0.42. Overall, the performance degradation does not seem to be very significant.

To better inform the comparisons, we have plotted the variations between the whole observed curves and the estimated ones. In Fig. 9 each line represents the difference, $\Delta\varepsilon_D$, between the predicted (regional in panel a; cross-validated in panel b) and observed ε_D for all durations D. Each curve refers to a specific station. Figure 9 shows that the performances in cross-validation are basically indistinguishable from those obtained with the pure regional model, in which the data of the "prediction" station are also used to fit the model. Panels (c) and (d) of the same Fig. 9 reports the relative errors obtained, that are bounded within ±10% for most of the basins and also for the longer durations. A slight underestimation bias must also be acknowledged.

The application of the CCA method produces average differences, in terms of FRF, that are even smaller, if we consider the 10-parameter model (results not shown). However, for some basins there are severe underestimates of the observed curve, exceeding 30% in a few cases, and which go over the 40% in cross-validation. For this reason, also considering the high number of parameters required, this method is deemed not so efficient in the domain of this regional analysis.

The application of the non-linear ACE models produces interesting results. In cross-validation, results confirm that the models with two descriptors are more robust than those with three independent variables. The passage from three to two descriptors also has a positive effect on the R^2_{adj} values.

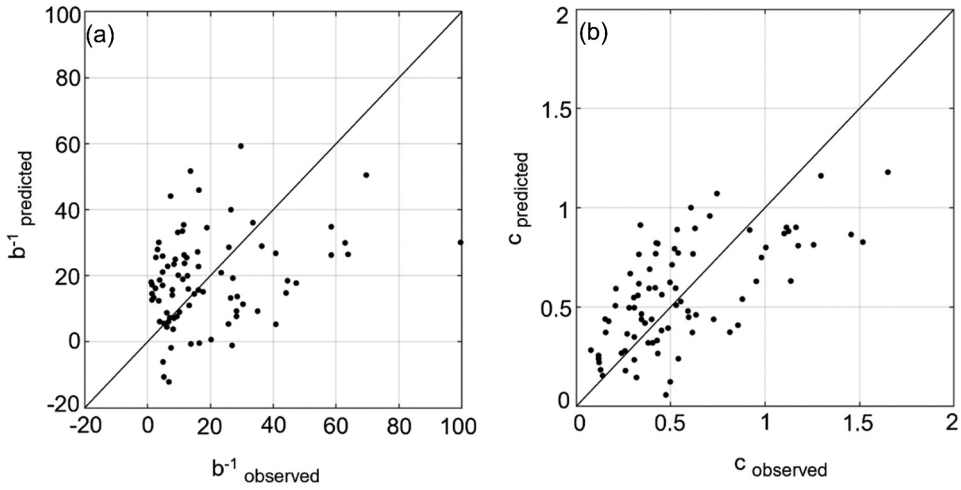

Figure 6. Values obtained from local estimates of (a) 1/b and (b) c versus those obtained from the Canonical Correlation Analysis regional model based on three descriptors (Table 4).

Table 5. Best Alternating Conditional Expectation algorithm models among all possible combinations of two and three descriptors ranked by $R^2_{adj.}$

ID	No. descriptors	y	x	Mapping functions	R^2_{adj}	RRMSE
1	3	c	H_{avg}, LDP,IDFn	*	0.6483	0.36
2	3	b^{-1}	A,H_{avg}, F_f	*	0.4881	0.70
3	2	c	H_{avg}, LDP	Fig. 7(a)	0.6115	0.39
4	2	b^{-1}	H_{avg}, LDP	Fig. 7(b)	0.4306	0.75

*For the sake of brevity, the mapping functions are not reported. They are available in Cordero (2019).

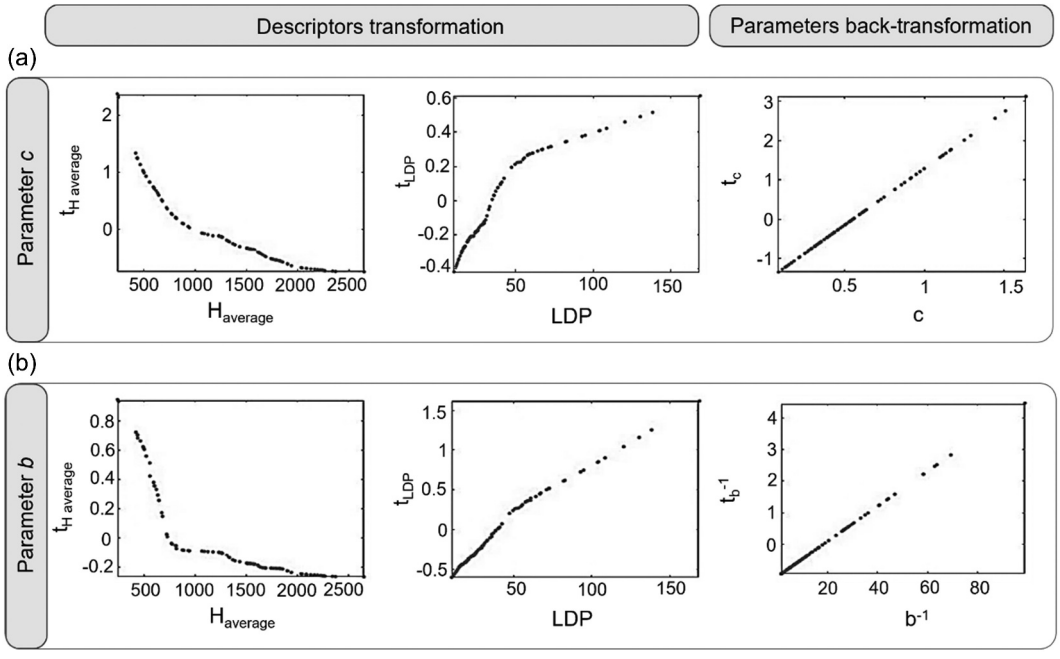

Figure 7. (a) The best Alternating Conditional Expectation algorithm model to estimate the flood reduction function c parameter among all possible combinations of two descriptors (ID 3 of Table 5); (b) the best Alternating Conditional Expectation algorithm model to estimate the flood reduction function b^{-1} parameter among all possible combinations of two descriptors (ID 4 of Table 5).

After cross-validation, the best model for parameter *c* is the two-descriptor one with R^2_{adj} = 0.5377 (for the three-descriptor model the R^2_{adj} is 0.525). The RRMSE remains almost constant between the three-variable and the two-variable models (from 0.43 to 0.42 for c and from 0.82 to 0.83 for b^{-1}).

The results of the FRF regional estimation for ACE models are shown in Fig. 10, where the panels (a) and (b) refer to the $\Delta\varepsilon_D$ curves computed before and after the cross-validation, respectively. Despite the high RRMSE of the individual parameter estimates, the overall errors on the FRF curve estimation remain limited.

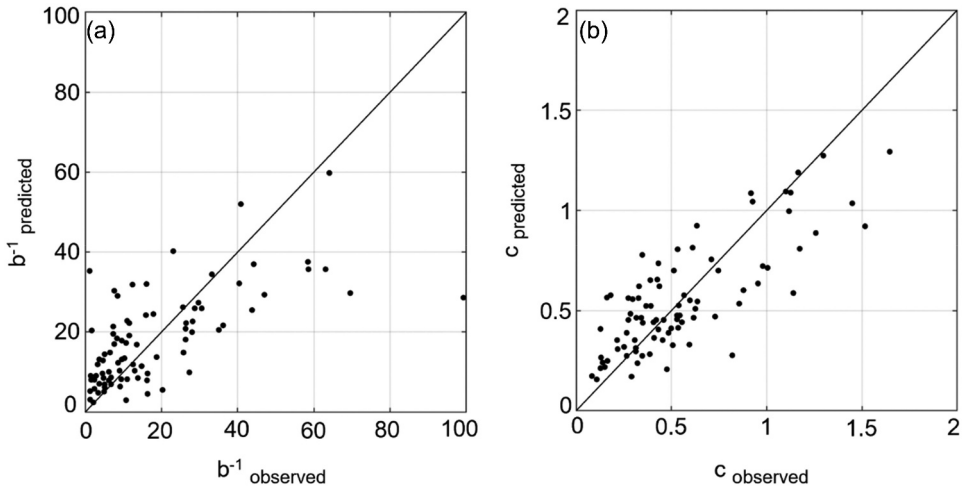

Figure 8. Estimated versus empirical values of parameters (a) 1/b and (b) c. Panel (a) uses the Alternating Conditional Expectation algorithm regional model for flood reduction function parameter 1/b (ID 4 in Table 5); panel (b) uses the Alternating Conditional Expectation algorithm regional model for flood reduction function parameter c (ID 3 in Table 5). See Table 2 for R^2_{adj} and RRMSE.

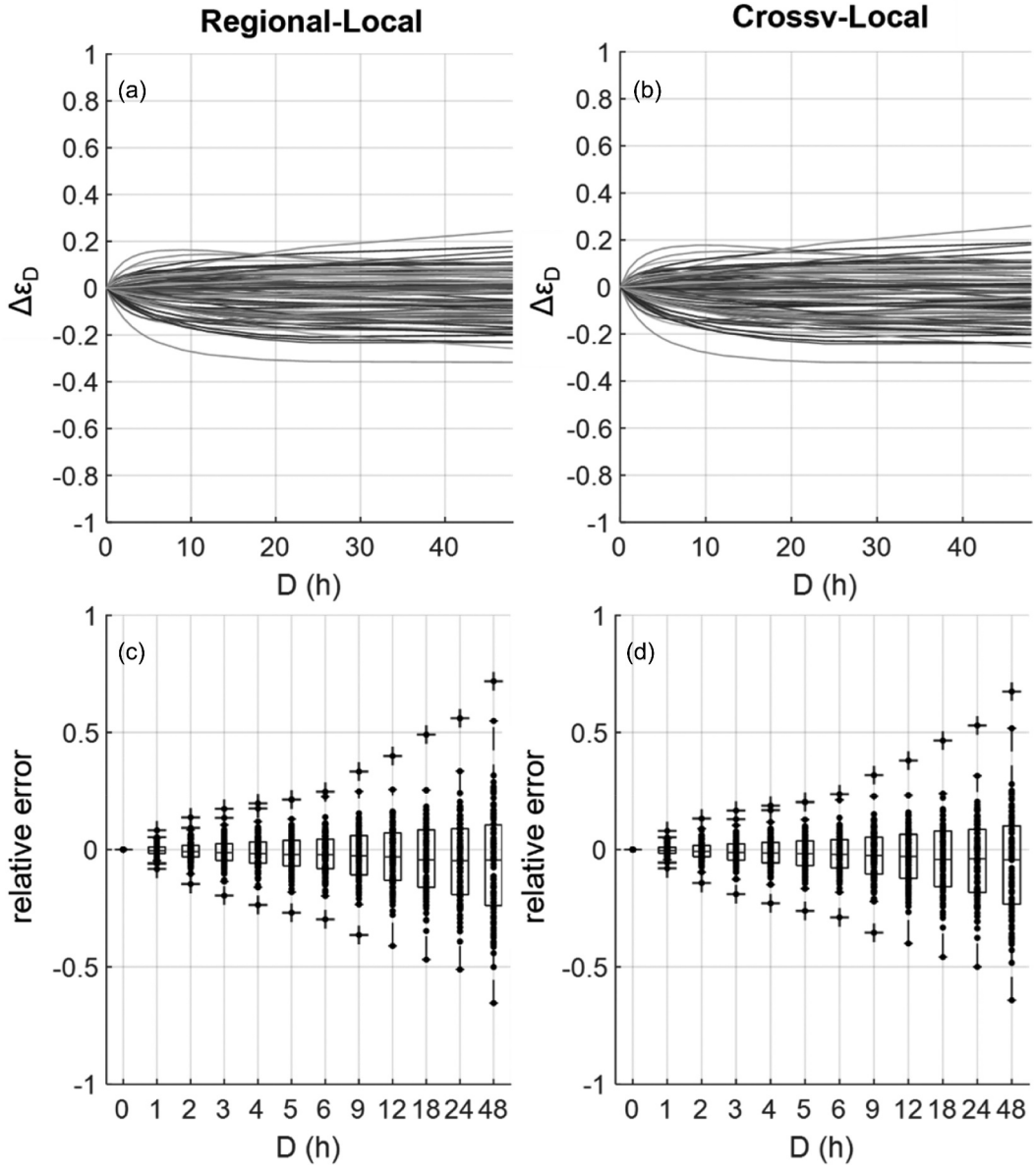

Figure 9. Regional estimation expressed by Equations (13) and (14) for flood reduction functions parameters 1/b and c, respectively. (a) difference between regionalized and observed flood reduction functions; (b) difference between regionalized after cross validation and observed flood reduction functions; (c) and (d) box plots of the relative error $\left(\varepsilon_{D,\ model} - \varepsilon_{D,\ observed}\right)/\varepsilon_{D,\ observed}$ for fitted flood reduction functions and regionalized flood reduction functions after cross-validation, respectively.

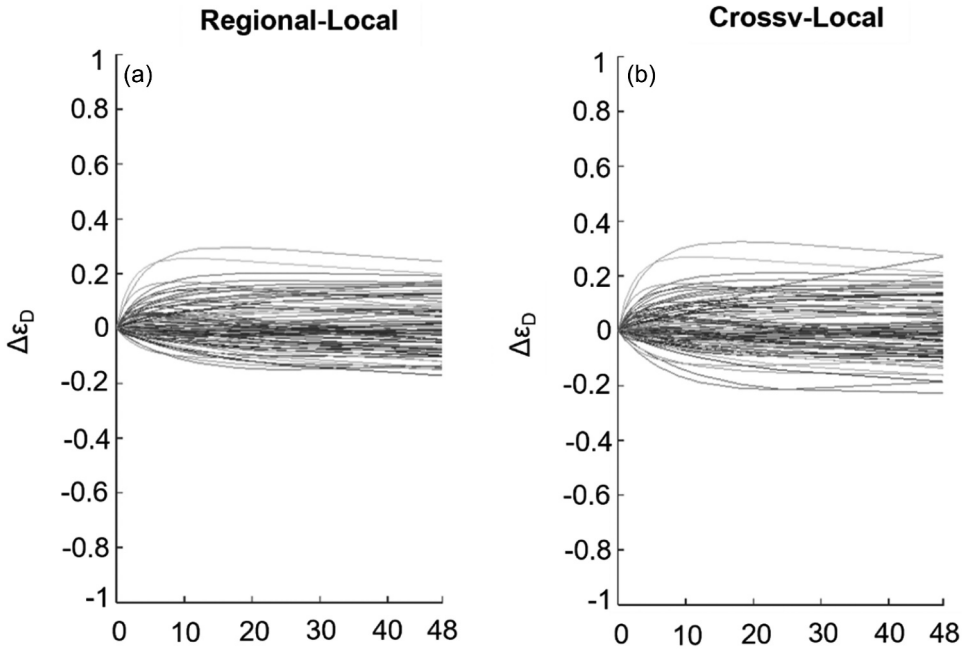

Figure 10. Results of the Alternating Conditional Expectation algorithm regional model: ID = 3 and ID = 4 from Table 5. The graphs report the differences, over the duration D, between: (a) regionalized and observed flood reduction functions, and (b) regionalized after cross-validation and observed flood reduction functions.

Summarizing the results obtained, the multiple linear regression globally leads to errors slightly larger than those obtained by ACE (compare Figs 9 and 10). However, the linear regression model is much easier to apply and less sensitive to extrapolation. To safely apply ACE models in extrapolation, the transformation curves should be first approximated with a polynomial of degree higher than 4, hence leading to a degradation of the model performances. The recommended models are, in conclusion, linear regressions with three descriptors.

4.1 Design hydrograph shape

As a final step of the analysis, we have evaluated the impact of the FRF estimation errors on the design hydrograph. We have compared the "regional" hydrograph (i.e. the one based on regionalized parameters) to a "reference" hydrograph, obtained from observations. As there is no established procedure to define what a "reference hydrograph shape" is, we have overlapped a sequence of suitable observed high-flow hydrographs, normalized by their peak value and centred around their time to peak. On this sample of standardized hydrograph shapes we have computed an average shape. The high-flow hydrographs were selected from the full-length discharge time series using a threshold so that the local peak is equal to or greater than 50% of the mean annual maximum of flow.

Using this approach, we have estimated the (constant) skew parameter r, by numerically minimizing the deviations between the FRF-based hydrograph and the empirical average shape.

After application of the regional analysis, two examples of comparisons are computed, as reported in Fig. 11. The regional hydrograph (dashed line) is plotted against the reference hydrograph (bold solid line); the thin lines represent the real recorded hydrographs (after standardization). In both cases the fitting is reasonably good, although in panel (a) one can notice that the regional hydrograph does not fit the quasi-convex shapes of the rising and falling limbs. However, if we consider the local NERC hydrograph (i.e. based on local parameters; dot-dashed line), we can notice that the FRF model itself is not fully adequate to represent the average hydrograph shapes. Sticking on the NERC model and fitting it to the observations, one can recognize that the regional hydrograph produces very good performance in reproducing the "local" NERC FRF function. Overall, almost all the investigated basins show a good fitting, and the maximum relative error of the regional estimates, computed in terms of differences between the area under the reference hydrograph and the one under the regional curve, does not exceed 30%. It is worth specifying that this procedure allows the empirical averaged normalized hydrograph to be fitted.

As regards the skew parameter *r*, we have computed it for all stations and have observed that it assumes rather constant values over the case study area. Slightly larger values of *r* only occurred for basins with higher average elevation. In a concrete application, we then suggest that the value of r can be taken from a neighbouring gauged basin, at least until a specific regional procedure is built for this parameter, which can be a matter for future investigation.

5 Conclusions

Flood hazard management and particularly the design of mitigation infrastructures requires accounting for the flood volume, in addition to the flood peak design value. However, statistical methods to estimate the flood volume or the shape of the flood hydrograph are still not consolidated, due to the conceptual difficulty in representing the hydrograph shape in

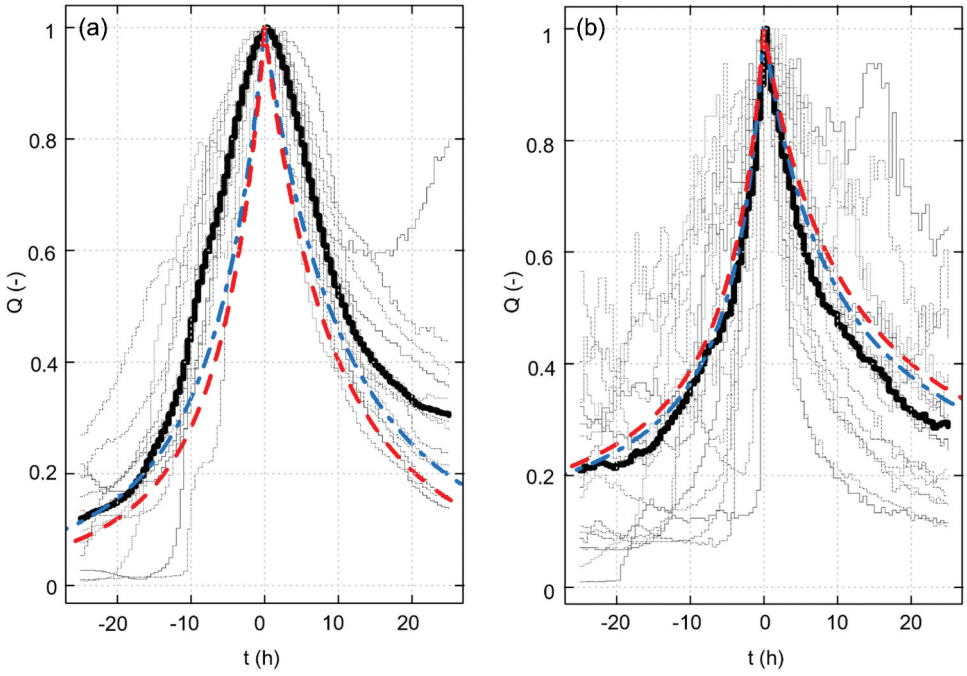

Figure 11. Comparison between Natural Environment Research Council synthetic flood hydrographs built using the proposed regional model (dashed curve) and the analytical flood reduction function (dot-dashed curve), compared to the empirical average hydrograph (bold solid curve). Bormida a Cassine watershed (code: BORCA, area 1516.25 km^2, mean elevation 493 m asl, r = 0.6) is shown in panel (a); Stura di Lanzo at Torino watershed (code: SLATO, area 879.97 km^2, mean elevation 1368 m asl, r = 0.68) is shown in panel (b).

a simple way and to the scarcity of data. These difficulties are exacerbated in ungauged basins. This paper addresses this problem by adopting the FRF as a powerful and parsimonious representation of the link existing between hydrograph volume and duration. The FRF can be used to "summarize" the hydrograph characteristics in a few parameters, easy to estimate even in ungauged basins, that are then used to build synthetic design hydrographs with minimal assumptions about their shape. The FRF approach can also be used in gauged basins to "regularize" a sequence of observed hydrographs and to allow one to compute, in a systematic and reproducible way, a single representative mean hydrograph shape.

The work presented here shows that a simple parametrization of the FRF function, known as the NERC function, can be regionalized, using a set of basin attributes derived from terrain analysis, land-use features and climatic indices. Different regionalization methods (multiple linear regression, canonical correlation analysis, alternating conditional expectation algorithms) were tested here, with the result that a rather simple multiple linear regression model can provide satisfactory estimation performances for the set of basins considered. The model uses as predictors easily available basin descriptors such as the length and slope of the longest drainage path, the mean basin elevation, the scaling exponent of the mean basin IDF curve and the kurtosis of the width function. The proposed model provides a good estimate of the empirical average FRF with R^2_{adj} values slightly lower than those obtained with more complex models. The use of the NERC regionalized parameters has also allowed us to assess the model capability to build synthetic hydrographs for each of the investigated basins, that have been compared to the average empirical hydrograph observed at the same gauging station.

In conclusion, with the reasonably good results obtained we have shown that the estimation of flood hydrographs in ungauged basins can be performed through regionalization techniques like those used for the frequency analysis of flood peaks, and with minimal additional assumptions. However, as the records of flood hydrographs are much shorter than the corresponding record of flow maxima, an effort to both collect new data and make available existing records is required to properly support all the practical applications that involve the management of flood volumes.

Acknowledgements

The authors acknowledge support from the EU Territorial Co-operation Program INTERREG (Alcotra), project RESBA-1729. ARPA Piemonte kindly provided the data and the original stream-gauge records.

Funding

This work was supported by the EU in the InterregV-A Italy-France European Territorial Co-operation Program (RESBA project - "RESiliencedesBArrages", project No 1729).

ORCID

Daniele Ganora http://orcid.org/0000-0003-0605-6200
Giulia Evangelista http://orcid.org/0000-0002-6188-6066
Pierluigi Claps http://orcid.org/0000-0002-9624-7408

Data availability statement

Data in support of this manuscript are available in a web GIS (www.resba.it).

References

Ayalew, D.W., *et al.*, 2022. An evidence for enhancing the design hydrograph estimation for small and ungauged basins in Ethiopia. *Journal of Hydrology: Regional Studies*, 42, 101123.

Bacchi, B., Brath, A., and Kottegoda, N.T., 1992. Analysis of the relationships between flood peaks and flood volumes based on crossing properties of river flow processes. *Water Resources Research*, 28 (10), 2773–2782. doi:10.1029/92WR01135.

Bacova Mitková, V. and Halmová, D., 2014. Joint modeling of flood peak discharges, volume and duration: a case study of the Danube River in Bratislava. *Journal of Hydrology and Hydromechanics*, 62 (3), 186–196. doi:10.2478/johh-2014-0026.

Bartolini, E., *et al.*, 2011. Analisi spaziale delle precipitazioni medie ed intense su Piemonte e Valle d'Aosta. *Working Paper 02*. Politecnico di Torino. Available from: http://www.idrologia.polito.it/~claps/Papers/wp_precipitazionipiemonte.pdf [Accessed 9 September 2022].

Blöschl, G., *et al.*, eds., 2013. *Runoff prediction in Ungauged basins: synthesis across processes, places and scales*. New York: Cambridge University Press.

Box, G.E.P. and Cox, D.R., 1964. An analysis of transformations. *Journal of the Royal Statistical Society, Series B (Methodological)*, 26 (2), 211–252. doi:10.1111/j.2517-6161.1964.tb00553.x.

Breiman, L. and Friedman, J.H., 1985a. Estimating optimal transformations for multiple regression and correlation. *Journal of the American Statistical Association*, 80 (391), 580–598. doi:10.1080/01621459.1985.10478157.

Breiman, L. and Friedman, J.H., 1985b. Estimating optimal transformations for multiple regression and correlation - rejoinder. *Journal of the American Statistical Association*, 80 (391), 614–619.

Brunner, M.I., *et al.*, 2017. Flood type specific construction of synthetic design hydrographs. *Water Resources Research*, 53 (2), 1390–1406. doi:10.1002/2016WR019535.

Brunner, M.I., *et al.*, 2018. Synthetic design hydrographs for ungauged catchments: a comparison of regionalization methods. *Stochastic Environmental Research and Risk Assessment*, 32 (7), 1993–2023. doi:10.1007/s00477-018-1523-3.

Castellarin, A., *et al.*, 2012. Review of applied-statistical methods for flood-frequency analysis in Europe, NERC/Centre for Ecology & Hydrology (ESSEM COST Action ES0901).

Chow, V.T., 1951. A general formula for hydrologic frequency analysis. *Eos, Transactions American Geophysical Union*, 32 (2), 231–237. doi:10.1029/TR032i002p00231.

Claps, P., *et al.*, 14–17 September 2010. Riesame ed integrazione di serie di portate al colmo mediante scale di deflusso di piena. In: *XXXII Convegno Nazionale Di Idraulica e Costruzioni Idrauliche*. Palermo, Italy: Walter Farina Editore.

Cordero, S., 2019. *Metodologie statistiche e sperimentali per il supporto ai piani di emergenza in presenza di invasi artificiali*. Thesis (PhD). Politecnico di Torino. Available from: https://iris.polito.it/handle/11583/2744152#.X8CzZC9aZZg [Accessed 9 September 2022].

Cunnane, C., 1988. Methods and merits of regional flood frequency-analysis. *Journal of Hydrology*, 100 (1–3), 269–290. doi:10.1016/0022-1694(88)90188-6.

Dalrymple, T., 1960. *Flood-frequency analyses. Manual of hydrology: part 3. Flood-flow techniques*. Usgpo 1543-A: 80. Available from: http://pubs.usgs.gov/wsp/1543a/report.pdf [Accessed 9 September 2022].

Farr, T.G., Rosen, P.A., and Caro, E., eds., 2007. The shuttle radar topography mission. *Reviews of Geophysics*, 45 (2), RG2004.doi:10.1029/2005RG000183.

Fiorentino, M., Rossi, F., and Villani, P., 1987. Effect of the basin geomorphoclimatic characteristics on the mean annual flood reduction curve. In: *Proceedings of the 18th annual Pittsburgh IASTED international conference,* Pittsburgh. Vol. 18, part 5, 1777–1784.

Franchini, M. and Galeati, G., 2000. Comparative analysis of some methods for deriving the expected flood reduction curve in the frequency domain. *Hydrology and Earth System Sciences*, 4 (1), 155–172. doi:10.5194/hess-4-155-2000.

Gallo, E., *et al.*, 2013. *Atlas of the piedmont watersheds (in Italian)*. Piedmont Region: Renerfor-Alcotra Project, 978-88-96046-06-7. Available from: http://www.idrologia.polito.it/web2/open-data/Renerfor/atlante_bacini_piemontesi_LR.pdf [Accessed 9 September 2022].

Grimaldi, S., *et al.*, 2011. Statistical hydrology. In: P. Wilderer, ed. *Treatise on water science*. Oxford: Academic Press, 479–517.

Grimaldi, S., *et al.*, 2022. Continuous hydrologic modelling for small and ungauged basins: a comparison of eight rainfall models for sub-daily runoff simulations. *Journal of Hydrology*, 610, 127866. doi:10.1016/j.jhydrol.2022.127866

Gumbel, E.J., 1945. Simplified plotting of statistical observations. *Eos, Transactions American Geophysical Union*, 26 (1), 69–82. doi:10.1029/TR026i001p00069.

Hastie, T., Tibshirani, R., and Friedman, J., 2009. *The elements of statistical learning: data mining, inference and prediction*. 2nd ed. New York: Springer.

Koutsoyiannis, D., Kozonis, D., and Manetas, A., 1998. A mathematical framework for studying rainfall intensity-duration-frequency relationships. *Journal of Hydrology*, 206 (1–2), 118–135. doi:10.1016/S0022-1694(98)00097-3.

Maione, U., Mignosa, P., and Tomirotti, M., 2003. Regional estimation of synthetic design hydrographs. *International Journal of River Basin Management*, 1 (2), 151–163. doi:10.1080/15715124.2003.9635202.

Mediero, L., Jiménez-Álvarez, A., and Garrote, L., 2010. Design flood hydrographs from the relationship between flood peak and volume. *Hydrology and Earth System Sciences*, 14 (12), 2495–2505. doi:10.5194/hess-14-2495-2010.

Montgomery, D., Peck, E., and Vining, G., 2001. *Introduction to linear regression analysis*. 3rd ed. Wiley Series Probability and Statistics. New York: Wiley.

Moré, J.J. and Sorensen, D.C., 1983. Computing a trust region step. *Journal on Scientific and Statistical Computing*, 4 (3), 553–572. doi:10.1137/0904038.

Mulvaney, T.J., 1851. On the use of self-registering rain and flood gauges in making observations of the relations of rainfall and flood discharges in a given catchment. *Transactions of the Institution of Civil Engineers of Ireland*, 4, 19–33.

Natural Environment Research Council, 1975. Estimation of flood volumes over different duration. *Flood Studies Report*, 1, 352–373.

Ouarda, T.B.M.J., *et al.*, 2000. Regional flood peak and volume estimation in northern Canadian basin. *Journal of Cold Regions Engineering*, 14 (4), 176–191. doi:10.1061/(ASCE)0887-381X(2000)14:4(176).

Ouarda, T., *et al.*, 2001. Regional flood frequency estimation with canonical correlation analysis. *Journal of Hydrology*, 254 (1–4), 157–1\73. doi:10.1016/S0022-1694(01)00488-7.

Petroselli, A. and Grimaldi, S., 2018. Design hydrograph estimation in small and fully ungauged basins: a preliminary assessment of the EBA4SUB framework. *Journal of Flood Risk Management*, 11, S197–S210. doi:10.1111/jfr3.12193

Requena, A.I., *et al.*, 2016. Extension of observed flood series by combining a distributed hydro-meteorological model and a copula-based model. *Stochastic Environmental Research and Risk Assessment*, 30 (5), 1363–1378. doi:10.1007/s00477-015-1138-x.

Salvadori, G. and De Michele, C., 2007. On the use of copulas in hydrology: theory and practice. *Journal of Hydrologic Engineering*,

12 (4), 369–380. doi:10.1061/(ASCE)1084-0699(2007)12:4(369).

Silvagni, G., 1984. *Valutazione dei massimi deflussi di piena*. Pubb. n. 489, Pubb. Ist. Idraulica, Univ. di Napoli.

Snyder, W.M., 1962. Some possibilities for multivariate analysis in hydrologic studies. *Journal of Geophysical Research*, 67 (2), 721–729. doi:10.1029/JZ067i002p00721.

Spector, P., *et al*., 2016. *ACE and AVAS for selecting multiple regression transformations* [Software]. CRAN. Available from: https://cran.r-project.org/package=acepack [Accessed 9 September 2022].

Tomirotti, M. and Mignosa, P., 2017. A methodology to derive synthetic design hydrographs for river flood management. *Journal of Hydrology*, 555, 736–743. doi:10.1016/j.jhydrol.2017.10.036

Villani, P., 2003. *Rapporto sulla valutazione delle piene in Piemonte*. Fisciano: Del Paguro, 89–118.

Wong, T.S., 1963. A multivariate statistical model for predicting mean annual flood in New England. *Annals of the Association of American Geographers*, 53 (3), 298–311. doi:10.1111/j.1467-8306.1963.tb00451.x.

Yue, S., *et al*., 1999. The Gumbel mixed model for flood frequency analysis. *Journal of Hydrology*, 226 (1–2), 88–100. doi:10.1016/S0022-1694(99)00168-7.

Yue, S., *et al*., 2002. Approach for describing statistical properties of flood hydrograph. *Journal of Hydrologic Engineering*, 7 (2), 147–153. doi:10.1061/(ASCE)1084-0699(2002)7:2(147).

Zhang, L. and Singh, V.P., 2006. Bivariate flood frequency analysis using the copula method. *Journal of Hydrologic Engineering*, 11 (2), 150–164. doi:10.1061/(ASCE)1084-0699(2006)11:2(150).

Appendix

Table A1. List of the geomorphological, climatological and soil descriptors used in the regional analyses.

Attribute category	Attribute	Notation	Unit	Description
Geomorphological	East coordinate of the basin's centroid (WGS84 UTM32N)	X_b	m	Reference system: WGS84 (EPSG code: 4326).
	North coordinate of the basin's centroid (WGS84 UTM32N)	Y_b	m	Reference system: WGS84 (EPSG code: 4326).
	Basin area	A	km^2	The area required for channel initiation has been set to 1 km^2.
	Basin mean elevation	H_{avg}	m a.s.l.	-
	Length of longest drainage path	LDP	km	Path included between the outlet and the point farthest from it, placed on the edge of the basin watershed and identified by following the drainage directions.
	Mean slope of longest drainage path	LDPs	-	Ratio of the difference between basin maximum and minimum elevation to the length of the longest drainage path.
	Drainage density	D_d	km^{-1}	Ratio of the total length of the river network to the basin area.
	Shape factor	F_f	-	Ratio of the basin area to the square of the length of the main channel.
	Width function kurtosis	Ku_{fa}	-	The width function is defined by counting the number of pixels having equal distance from the gauging station. This distance is measured following the drainage path. The 4^{th} statistical moment of the width function has been computed.
	Slope ratio	R_s	-	Ratio of average slope of streams of two adjacent orders *u* and *u* + *1*. Streams are numbered according to Horton's criterion.
Climatological	Mean a parameter of the IDF curve	IDF_a	mm h^{-1}	Scale factor of the intensity-duration-frequency curve. The average value over the basin area has been calculated.
	Mean n parameter of the IDF curve	IDF_n	-	Scaling exponent of the intensity-duration-frequency curve. The average value over the basin area has been calculated.
	Mean coefficient of L-skewness for 3-hours duration	Lca3h	-	Coefficient of L-skewness for 3-hours duration. The average value over the basin area has been calculated.
	Mean coefficient of L-skewness for 12-hours duration	Lca12h	-	Coefficient of L-skewness for 12-hours duration. The average value over the basin area has been calculated.
	Mean annual precipitation over the basin	MAP	mm	Total mean annual precipitation (Bartolini *et al*. 2011).
	Spatial coefficient of variation of the mean annual precipitation	cv [MAP]	mm	-
	Coefficient of variation of the rainfall regime over the basin	cv [rr]	-	Calculated from the 12 mean monthly rainfall depths, computed using monthly data from Bartolini *et al*. (2011).
	Mean Fourier coefficient B2 of the rainfall regime	$Fourier_{B2}$	-	Mean values of the B2 coefficient of the Fourier series representation of the rainfall regime. The reader can refer to Gallo *et al*. (2013) for details about the meaning of the B2 coefficient.
Soil	Mean permeability index	c_f	%	Permeability index used in the Vapi project (Villani 2003). This coefficient has been obtained by classification of permeability values in flood conditions by balancing the rational equation. The average value over the basin area has been calculated.